POST-BUCKLING BEHAVIOUR OF SLENDER STRUCTURES WITH A BI-LINEAR BENDING MOMENT - CURVATURE RELATIONSHIP

M. A. VAZ[1] and M. H. PATEL[2]

1. Ocean Engineering Department, Graduate School of Engineering
Federal University of Rio de Janeiro
P.O. Box 68508, 21945-970, Rio de Janeiro – RJ, Brazil
2. School of Engineering, Cranfield University
Cranfield, Bedfordshire, MK43 0AL
United Kingdom

International Journal of Non-linear Mechanics, Vol 42, p 470-483, 2007.

ABSTRACT

Certain classes of slender structures of complex cross-section or fabricated from specialized materials can exhibit a bi-linear bending moment – curvature relationship that has a strong influence on their global structural behaviour. This condition may be encountered, for instance, in (a) non-linear elastic or inelastic post-buckling problems if the cross-section stiffness may be well approximated by a bi-linear model; (b) multi-layered structures such as stranded cables, power transmission lines, umbilical cables and flexible pipes where the drop in the bending stiffness is associated with an internal friction mechanism. This paper presents a mathematical formulation and an analytical solution for such slender structures with a bi-linear bending moment versus curvature constitutive behaviour and subjected to axial terminal forces. A set of five first-order non-linear ordinary differential equations are derived from considering geometrical compatibility, equilibrium of forces and moments and constitutive equations, with hinged boundary conditions prescribed at both ends, resulting a complex two-point boundary value problem. The variables are non-dimensionalised and solutions are developed for monotonic and unloading conditions. The results are presented in non-dimensional graphs for a range of critical curvatures and reductions in bending stiffness, and it is shown how these parameters affect the structure's post-buckling behaviour.

Keywords: elastica, rod post-buckling, slender rods.

1. INTRODUCTION

The structural mechanics of complex layered structures is governed by internal physical mechanisms that have non-linear force versus displacement relationships. In most practical instances, such behaviour has a small influence on the global behaviour of the structure and engineering analysis can be carried out using linearised constitutive equations. However, as the complexity of the layered structure increases and the loading application becomes more demanding, this simplified approach breaks down and leads to significant and unacceptable errors in design analysis.

Once such case is that of flexible pipes, umbilicals and marine cables used in the exploration of oil and gas deposits under the sea-bed in very deep water (1000 to 2000 m depth).

These are slender structures of between 0.1 and 0.75 m in diameter and up to 3000m in length – freely suspended in the water column or laying on the sea bed. The internal composition of these structures is a combination of cylindrical elastomer sheaths and fluid barriers combined

with helically wound armour wire or bar layers and in some cases helically wound inter-linked carcass strips. The interface between the layers relies only on contact forces with radial pressure transmission and tangential or axial friction forces being the only mechanisms that are in play.

The structural mechanics of these complex layered structures has been extensively studied. It is characterised by four principal phenomena as follows:

1. The structure exhibits a bi-linear hysteretic bending moment against curvature relationship arising from the progressive activation of friction and consequential slipping between adjacent layers.
2. Torsional and tensile forces and deflection are coupled due to the structural behaviour of the helical armour wires.
3. The torsional movement against twist relationship is bi-linear and arises from the locking or un-locking of the helical armour wires due to the direction of twist.
4. The axial stiffness is asymmetric for tensile and compressive loads as the armour wires encounter different resistance to inward and outward radial displacements.

As the oil industry has pushed the deployment of these structures towards increasing water depth, the influence of the above effects on global behaviour and possible failure has become more important.

These slender structures are used in deep water within catenaries at relatively low tension where dynamic effects can induce transient compression forces. At the same time, the effect of very high external hydrostatic pressure in deep water is to induce a so called ‘effective tension’ term that is identical in its physical effects to a compressive loading on the structure. Seyed and Patel (1992) describe the formulation and effect of this ‘effective tension’ term. A further issue is the axial-torsional coupled behaviour of these structures that, at low cyclic tension, can lead to looping instabilities which are influenced by the ratio of tensile to torsional stiffness. Tan and Witz (1993 and 1995) give an analysis of this but only using a linearised stiffness and ignoring bi-linear force-displacement relationships.

There is an extensive body of research literature characterising the structural behaviour of slender structures with helically wound armour layers. This has been built upon the work of Love (1944) setting out a definitive derivation of equilibrium equations for curved and helically wound rods. Although Love's equations are complex and difficult to solve analytically, an alternative approach was suggested by Lutchansky (1969), which directly calculates the deformation states of the helical elements according to different geometrical configurations before and after loading. Spillers et al (1983) followed a similar approach to investigate the mechanical behaviour of a helical tape on a bent cylinder. This work was continued by Oliveira et al (1985) who used Timoshenko's (1956, 1964) formulae, describing the bending stiffness of a spring with a large helical angle, to evaluate the bending stiffness of helical armour layers. Oliveira et al neglected the effects of friction and cylindrical restriction - these are important aspects of the behaviour of such unbonded layered structures. The corresponding results are questionable since the helical angle of the armour layers is not usually large enough for Timoshenko's formulae to be applicable. Other contributions to the field have been made by Costello and Phillips (1976), Costello (1977), Le Clair and Costello (1986), Féret and Bournazel (1987), Out (1989), Harte and McNamara (1990), McNamara and Harte (1992), Saevik (1992), McIver (1992) and Custódio and Vaz (2002) for both axial - torsional loads and bending of these flexible structures.

However, much of the early work neglected the combined effects of inter-layer friction and cylindrical restriction which are an essential ingredient to accurately model the structural behaviour of helically armoured structures. This problem has been addressed by Witz and Tan (1992a, 1992b), Tan et al (1991) and Pearson et al (1993) to arrive at a mathematical formulation that includes friction and cylindrical restriction effects. The non-linear difficulty of the problem is resolved by deriving complex equilibrium equations that describe the behaviour of each helical and cylindrical layer. These equations are in a form that can be solved by a numerical scheme that takes account of friction and cylindrical restrictions and deals with axial variations along the structure's length. This approach has the advantage of not requiring empirical coefficients, these being a feature of the models of Knapp (1975, 1988, 1989) and Feld (1992). Internal friction has a significant influence on the apparent bending stiffness of the pipe - see Raoof and Huang (1992), Feld (1992), and Witz and Tan (1992b).

The stability in buckling of a slender, homogenous rod was first addressed by Euler in 1744. This has been followed up by a substantial body of work that considers the post-buckling problem. Usually a perturbation expansion technique is used for insight into the initial post-buckling response for the type of equilibrium achieved. Asymptotic solutions also enable analytical investigation on extreme conditions. However, recent advances in numerical processing capability have allowed solution of complex post-buckling configurations, involving geometrical and physical non-linearities.

The elastica solutions via elliptical integrals are presented, for instance, in Timoshenko and Gere (1961) and Shames and Dym (1991), respectively for encastré and double-hinged rods. The search for post-buckled equilibrium configurations in slender rods still attracts considerable attention, given the gamut of boundary conditions, load fields, cross-section geometry, type of material etc, see recent works, for instance, from Theocaris and Panayotounakos (1982), Stemple (1990), Lee et al (1993), Koenig and Bolle (1993), Lu and Perkins (1995), Heinen and Fischer (1998), Gottlieb and Perkins (1999) and Lee and Oh (2000).

Boundary conditions play an important role in the buckling and post-buckling response as they indicate the degree of the system stiffness. Wang (1997) presents a solution for asymmetric boundary conditions employing a shooting method for numerically integrating the set of governing equations for an initially perfectly straight rod. In addition initial post-buckling and extreme load analyses are respectively dealt with by perturbation and asymptotic expansions. Vaz and Silva (2003) extend Wang's work by considering a rotational spring so a solution is obtained from double-hinged to hinged-built-in end conditions.

Initial geometric imperfections are known to play an important role in the buckling and post-buckling behaviour in many stability phenomena, see Tauchert and Lu (1987), but this effect is not investigated in this paper.

This paper is concerned with developing a methodology for the buckling and post-buckling behaviour of a slender structure with a bi-linear bending moment versus curvature property. A generalized solution is used to show the variation of displacement behaviour that can arise. This generalized methodology is an intermediate step towards more representative modeling of the global behaviour of slender structures that have bi-linear bending moment characteristics and are subjected to cyclic tensile and compressive loadings.

2. THE MATHEMATICAL FORMULATION

Consider a homogeneous, inextensible and initially straight rod with length L subjected to a perfectly centered axial load P, as shown in figure 1a. As the load is progressively increased the rod becomes unstable and buckles laterally at a critical load followed by large post-buckled deflections as the load is increased further. For linear elastic isotropic materials and assuming a pure bending cross-section behaviour, the critical buckling load is given by $P_{cr} = \pi^2 EI/L^2$, where E is the Young's Modulus and I is the principal minimum inertia of the cross-section area. Furthermore, a closed form analytical solution via elliptical integrals is available for description of the post-buckled regime. This latter problem is referred to in this paper as simple elastica. Now let's assume that the bending moment versus curvature of the rod exhibits bi-linear behaviour, that is, the rod cross-section bending stiffness is substantially reduced after a given critical curvature is reached. This paper aims to consistently investigate the effect of the loss of bending stiffness in the post-buckled configuration of such slender rods.

Figure 1a indicates that the curvature distribution in the rod ranges from zero at $S = 0$ (point O) to a maximum value at $S = L/2$ (point B). If this maximum curvature is smaller than the critical curvature the post-buckled configuration is described by an analytical solution. However, when the critical curvature reaches point B for a certain load (or end angle β, or free end displacement Δ) the rod starts "yielding", and two regions with different constitutive relations will take place. The segment OA, herein referred by the index $i = 1$, remains stiff, whereas segment AB ($i = 2$) will be subjected to a smaller bending stiffness and is then more "flexible". Continuity conditions must be assured at point A ($S = \gamma L$), where the parameter γ, $0 < \gamma \leq 1/2$, defines the transition point. Furthermore note that the curvature is critical at the transition point.

Classically, a mathematical model that describes the rod equilibrium configuration may be constructed from geometrical compatibility, equilibrium of forces and moments and constitutive relations applied to an infinitesimal rod element, depicted in figure 1b. Note that there is no force component in the Y - axis direction since no distributed load is considered and the boundary conditions are assumed hinged-hinged.

Geometrical Compatibility

The trigonometrical relations in the rod infinitesimal element dS (see figure 1b) yield:

$$\frac{dX_i}{dS} = \cos(\theta_i) \tag{1a}$$

$$\frac{dY_i}{dS} = \sin(\theta_i) \tag{1b}$$

Where S is the rod arch-length ($0 \leq S \leq L$), (X_i, Y_i) are the Cartesian coordinates of the post-buckled rod and θ_i is the angle between the tangent of the deflected rod centroid and the X - axis. Note that due to the symmetrical nature of the problem the material domain may be limited to $0 \leq S \leq L/2$. Consequently regions $i = 1$ and $i = 2$ are respectively defined for $0 \leq S \leq \gamma L$ and $\gamma L < S \leq L/2$. From differential geometry the curvature K_i is defined as:

$$\frac{d\theta_i}{dS} = \mathrm{K}_i \tag{1c}$$

Equilibrium of Forces and Moments

A schematic of the internal forces and moments in the rod infinitesimal element is also shown in figure 1b. The equilibrium of forces and bending moment respectively yields:

$$\frac{dP_i}{dS} = 0 \tag{2a}$$

$$\frac{dM_i}{dS} = P_i \sin(\theta_i) \tag{2b}$$

Where P_i is the force component in the X - axis direction and M_i is the bending moment.

Constitutive Relations

The rod cross-section presents a bi-linear bending moment versus curvature relation, see figure 2. This constitutive condition is typical in un-bonded layered structures such as umbilical cables and flexible pipes, for instance, where the rod cross-section at a first moment exhibits a large bending stiffness before a critical curvature is reached, and from this point the bending stiffness is significantly reduced. This mechanism originates when the bent helical layers are initially impeded to displace laterally due to Coulomb friction, as described by Witz and Tan (1992b), Féret et al (1995) and Leroy and Estrier (2001). -Note also that a Bernoulli-Euler pure bending condition is also considered herein. Hence:

$$M_1 = EI\ \mathrm{K}_1 \qquad if \quad \mathrm{K}_1 \le \mathrm{K}_{cr} \tag{3a}$$

$$M_2 = \alpha\ EI\ \mathrm{K}_2 + EI\ \mathrm{K}_{cr}\ (1-\alpha) \qquad if \quad \mathrm{K}_2 > \mathrm{K}_{cr} \tag{3b}$$

Where EI is the initial bending stiffness, K_{cr} is the critical curvature and α is the reduction factor for the secondary $M-\mathrm{K}$ curve.

Therefore, substituting equations (3a) and (3b) into (2b) results:

$$\frac{d\mathrm{K}_1}{dS} = \frac{P_1}{EI}\sin(\theta_1) \qquad if \quad \mathrm{K}_1 \le \mathrm{K}_{cr} \tag{4a}$$

$$\frac{d\mathrm{K}_2}{dS} = \frac{P_2}{\alpha\ EI}\sin(\theta_2) \qquad if \quad \mathrm{K}_2 > \mathrm{K}_{cr} \tag{4b}$$

Full Unloading

When the load is completely removed a residual and permanent deformation develops if any point of the rod exceeds the critical curvature. The unloading process may follow paths A or B (figure 2), depending on the value of the rod initial curvature. This constitutive behaviour has been observed experimentally in bending tests for flexible pipes and umbilical cables. Assuming that the unloading follows the initial stiffness, then:

$$\mathrm{K}_{1f} = 0 \qquad if \quad \mathrm{K}_1 \le \mathrm{K}_{cr} \tag{5a}$$

$$\mathrm{K}_{2f} = (1-\alpha)(\mathrm{K}_{2i} - \mathrm{K}_{cr}) \qquad if \quad \frac{(1+\alpha)}{\alpha}\mathrm{K}_{cr} \ge \mathrm{K}_2 > \mathrm{K}_{cr} \tag{5b}$$

$$\mathrm{K}_{2f} = \frac{(1-\alpha)}{\alpha}\mathrm{K}_{cr} \qquad if \quad \mathrm{K}_2 > \frac{(1+\alpha)}{\alpha}\mathrm{K}_{cr} \tag{5c}$$

Equation (5a) indicates that the cross-section returns to its non-deformed state if the critical curvature is not exceeded. Equations (5b) and (5c) respectively represent paths A and B, which are governed by a transition curvature defined by $\mathrm{K}_T = (1+\alpha)/\alpha\ \mathrm{K}_{cr}$. If the cross-section curvature reaches a value within the critical and transition curvatures the unload path A is followed. For any value above the transition curvature path B is observed.

Partial Unloading
The bending moment versus curvature relationship for partial unloading is given by:

$$M_{1u} = EI\ \mathrm{K}_{1u} \qquad if \quad \mathrm{K}_{1u} \le \mathrm{K}_{cr} \tag{5d}$$

$$M_{2u} = EI\ [\mathrm{K}_{2u} + (1-\alpha)(\mathrm{K}_{cr} - \mathrm{K}_{2i})] \qquad if \quad \frac{(1+\alpha)}{\alpha}\mathrm{K}_{cr} \ge \mathrm{K}_{2i} > \mathrm{K}_{cr} \tag{5e}$$

$$M_{2u} = EI\ [\alpha\,\mathrm{K}_{2u} - (1-\alpha)\mathrm{K}_{cr}] \qquad if \quad \mathrm{K}_{2i} > \frac{(1+\alpha)}{\alpha}\mathrm{K}_{cr} \tag{5f}$$

Where the subscript u merely indicates an unloading process.

Boundary Conditions
The boundary conditions for the double-hinged rod and continuity conditions at point A may be specified as:

$$X_1(0) = Y_1(0) = \theta_1(0) - \beta = \mathrm{K}_1(0) = P_1(0) - P = 0 \tag{6a}$$

$$X_1(\gamma L) - X_2(\gamma L) = Y_1(\gamma L) - Y_2(\gamma L) = \theta_1(\gamma L) - \bar{\theta} = \theta_2(\gamma L) - \bar{\theta} = 0 \tag{6b}$$

$$P_1(\gamma L) - P = P_2(\gamma L) - P = \mathrm{K}_1(\gamma L) - K_{cr} = \mathrm{K}_2(\gamma L) - K_{cr} = 0 \tag{6c}$$

$$\theta_2(L/2) = P_2(L/2) - P = 0 \tag{6d}$$

Where β and $\bar{\theta}$ are respectively the angles at points O and A. From equation (2a) it is seen that the force P is constant. The effect of any other boundary conditions on the rod buckling and post-buckling response is significant and it may be explored using a numerical methodology.

The Governing Equations
It is obviously convenient to reduce the set of differential equations (1a), (1b), (1c), (2a), (4a) or (4b) to a non-dimensional form using the following change of variables: $s = S/L$,

$x = X/L$, $y = Y/L$, $p = PL^2/EI$ and $\kappa = \mathrm{K}\, L$, where $0 \le s \le 1$. Hence the governing equations may be rewritten as:

$$\frac{dx_i}{ds} = \cos(\theta_i) \tag{7a}$$

$$\frac{dy_i}{ds} = \sin(\theta_i) \tag{7b}$$

$$\frac{d\theta_i}{ds} = \kappa_i \tag{7c}$$

$$\frac{dp_i}{ds} = 0 \tag{7d}$$

$$\frac{d\kappa_1}{ds} = p_1 \sin(\theta_1) \tag{7e}$$

or

$$\frac{d\kappa_2}{ds} = \frac{p_2}{\alpha} \sin(\theta_2) \tag{7f}$$

Where the non-dimensional variables (x_i, y_i) constitute the deflected rod Cartesian coordinates, s the arc-length, κ_i the curvature, θ_i the angle formed by the curve tangent and the longitudinal x-axis, p_i the longitudinal load and α the bending stiffness reduction factor.

Furthermore the boundary conditions given by equations (6a-d) may be also made non-dimensional:

$$x_1(0) = y_1(0) = \theta_1(0) - \beta = \kappa_1(0) = p_1(0) - p = 0 \tag{8a}$$

$$x_1(\gamma) - x_2(\gamma) = y_1(\gamma) - y_2(\gamma) = \theta_1(\gamma) - \overline{\theta} = \theta_2(\gamma) - \overline{\theta} = 0 \tag{8b}$$

$$p_1(\gamma) - p = p_2(\gamma) - p = \kappa_1(\gamma) - \kappa_{cr} = \kappa_2(\gamma) - \kappa_{cr} = 0 \tag{8c}$$

$$\theta_2(1/2) = p_2(1/2) - p = 0 \tag{8d}$$

Hence the influence of the critical curvature κ_{cr} ($\kappa_{cr} = L\,\mathrm{K}_{cr}$) and the bending stiffness reduction factor α on the rod post-buckled deflected configuration may be analytically calculated.

3. POST-BUCKLING SOLUTIONS

3.1 Analytical Solution for Monotonic Loading

For a given κ_{cr} it is possible to calculate, employing elliptical integrals, the critical values for the end angle, load, maximum deflection and support longitudinal displacement, respectively β_{cr}, $\overline{p}_{cr}$, $y_{\max}$ and δ_{cr}. From this point part of the rod will progressively "yield".

Substituting equation (7c) in (7e) and (7f) respectively gives:

$$\frac{d^2\theta_1}{ds^2} = p\sin(\theta_1) \qquad if \qquad 0 \le s \le \gamma \tag{9a}$$

$$\frac{d^2\theta_2}{ds^2} = \frac{p}{\alpha}\sin(\theta_2) \qquad if \qquad \frac{1}{2} \ge s > \gamma \tag{9b}$$

Integrating equation (9a) and applying appropriate boundary conditions yields:

$$\frac{d\theta_1}{ds} = \pm\sqrt{2p\left[\cos(\theta_1) - \cos(\beta)\right]} \qquad if \qquad 0 \le s \le \gamma \tag{10}$$

The sign choice in equation (10) is arbitrary as it only changes the quadrant for the deflected rod. Furthermore the curvature in point A is κ_{cr} and the angle is $\bar{\theta}$, hence:

$$\kappa_{cr} = \pm\sqrt{2p\left[\cos(\bar{\theta}) - \cos(\beta)\right]} \tag{11}$$

Substituting $c = \sin(\beta/2)$ and $\sin(\theta_1/2) = c\sin(\phi_1)$ in equation (10) and integrating it after some algebraic manipulation gives:

$$\gamma = -\frac{\sqrt{2\left[\cos(\bar{\theta}) - \cos(\beta)\right]}}{|\kappa_{cr}|}\int_{\pi/2}^{\bar{\phi}} \frac{d\phi_1}{\sqrt{1 - c^2\sin^2(\phi_1)}} \tag{12}$$

Where:

$$\bar{\phi} = \sin^{-1}\left[\frac{\sin(\bar{\theta}/2)}{\sin(\beta/2)}\right]$$

This change of variable is necessary to avoid singularity. Now, integrating equation (9b) and applying adequate boundary conditions gives:

$$\frac{d\theta_2}{ds} = \pm\sqrt{\frac{2p}{\alpha}\left[\cos(\theta_2) - \cos(\bar{\theta})\right] + \kappa_{cr}^2} \qquad if \qquad \frac{1}{2} \ge s > \gamma \tag{13}$$

Integrating equation (13) after trigonometric manipulation yields:

$$\frac{1}{2} - \gamma = -\frac{\sqrt{\alpha\left[\cos(\bar{\theta}) - \cos(\beta)\right]}}{|\kappa_{cr}|}\int_{\bar{\theta}}^{0} \frac{d\theta_2}{\sqrt{\cos(\theta_2) - (1-\alpha)\cos(\bar{\theta}) - \alpha\cos(\beta)}} \tag{14}$$

Adding equations (12) and (14) results in:

$$|\kappa_{cr}| = \sqrt{\cos(\bar{\theta}) - \cos(\beta)} \left[\int_{\bar{\phi}}^{\pi/2} \frac{2\sqrt{2}\, d\xi}{\sqrt{1 - c^2 \sin^2(\xi)}} + \int_{0}^{\bar{\theta}} \frac{2\sqrt{\alpha}\, d\xi}{\sqrt{\cos(\xi) - (1-\alpha)\cos(\bar{\theta}) - \alpha\cos(\beta)}} \right] \qquad (15)$$

For a known κ_{cr} and α the angle in the transition point A, $\bar{\theta}$, is calculated from equation (15) for each angle β. As a direct solution is difficult an interpolation procedure was developed with Matlab (2002) by varying the angle $\bar{\theta}$ until the critical curvature was found. Then the load, p, and position of the transition point A, γ, may be readily obtained from equations (11) and (12), respectively. It must be pointed out that this solution is correct as long as no material point experiences reduction in curvature.

The Cartesian coordinates

The coordinates of the deflected rod may be obtained from integrating equations (7a-b):

The x - coordinates

$$x_1(s) = -\frac{1}{\sqrt{p}} \int_{\pi/2}^{\phi_1} \frac{1 - 2c^2 \sin^2(\xi)}{\sqrt{1 - c^2 \sin^2(\xi)}} d\xi \qquad (16a)$$

Where:

$$\phi_1 = \sin^{-1}\left[\frac{\sin(\theta_1/2)}{\sin(\beta/2)} \right]$$

$$\beta \geq \theta_1 \geq \bar{\theta}$$

$$\frac{\pi}{2} \geq \phi_1 \geq \bar{\phi}$$

Then $x_1(\gamma)$ can be easily calculated when $\phi_1 = \bar{\phi}$ in equation (16a), and the coordinates $x_2(s)$ are then:

$$x_2(s) = x(\gamma) - \frac{\sqrt{\alpha\,[\cos(\bar{\theta}) - \cos(\beta)]}}{|\kappa_{cr}|} \int_{\bar{\theta}}^{\theta_2} \frac{\cos(\xi)\ \ d\xi}{\sqrt{\cos(\xi) - (1-\alpha)\cos(\bar{\theta}) - \alpha\cos(\beta)}} \qquad (16b)$$

Where $\bar{\theta} \geq \theta_2 \geq 0$

The y - coordinates

$$y_1(s) = \mp \frac{2c}{\sqrt{p}} \cos(\phi_1) \qquad (16c)$$

Then $y_1(\gamma)$ can be easily calculated for $\phi_1 = \bar{\phi}$ in equation (16c). The coordinates $y_2(s)$ are then:

$$y_2(s) = y(\gamma) \mp \frac{\sqrt{\alpha\,[\cos(\bar{\theta}) - \cos(\beta)]}}{|\kappa_{cr}|} \int_{\bar{\theta}}^{\theta_2} \frac{\sin(\xi)\;\; d\xi}{\sqrt{\cos(\xi) - (1-\alpha)\cos(\bar{\theta}) - \alpha\cos(\beta)}} \tag{16d}$$

Note also that $\kappa_{cr} = -p\, y_1(\gamma)$ and $\kappa_{\max} = \dfrac{(\alpha - 1)\kappa_{cr} - p\, y_{\max}}{\alpha}$.

3.2 Numerical Solutions for Unloading
Full Unloading Analysis

In this section a methodology is sought to describe the rod final residual configuration when load is fully removed. For the unloading schemes presented in Figure 2 the rod final curvature κ_{1f} and κ_{2f} are respectively:

$$\kappa_{1f} = 0 \qquad if \qquad k_{1i} \le k_{cr} \tag{17a}$$

$$\kappa_{2f} = (1-\alpha)(\kappa_{2i} - \kappa_{cr}) \qquad if \qquad k_{cr} < k_{2i} \le \frac{(1+\alpha)}{\alpha} k_{cr} \tag{17b}$$

$$\kappa_{2f} = \frac{(1-\alpha)}{\alpha}\kappa_{cr} \qquad if \qquad k_{2i} > \frac{(1+\alpha)}{\alpha} k_{cr} \tag{17c}$$

Where κ_{2i} indicates the curvature distribution after a monotonic increasing load is applied. Then the final angle distribution may be numerically calculated integrating equation (7c) and considering that $\theta_{2f}(1/2) = 0$:

$$\theta_{2f}(s) = \int_s^{1/2} \kappa_{2f}(s)\, ds \qquad \gamma < s \le \frac{1}{2} \tag{18a}$$

The angle in the first rod segment is constant and given by:

$$\theta_{1f}(s) = \theta_{2f}(\gamma) \qquad 0 \le s \le \gamma \tag{18b}$$

The Cartesian coordinates may now be calculated from equations (7a) and (7b):

$$x_{1f}(s) = s\,\cos[\theta_{1f}(s)] \qquad 0 \le s \le \gamma \tag{19a}$$

$$y_{1f}(s) = s\,\sin[\theta_{1f}(s)] \qquad 0 \le s \le \gamma \tag{19b}$$

$$x_{2f}(s) = x_{1f}(\gamma) + \int_s^{1/2} \cos[\theta_{2f}(s)]\, ds \qquad \gamma < s \le \frac{1}{2} \tag{19c}$$

$$y_{2f}(s) = y_{1f}(\gamma) + \int_{s}^{1/2} \sin[\theta_2(s)]\, ds \qquad \gamma < s \le \frac{1}{2} \tag{19d}$$

Equations (19c-d) may be numerically calculated.

Partial Unloading Analysis

Making equations (5d-f) non-dimensional and differentiating them with respect to the arc-length respectively yields:

$$\frac{dk_{1u}}{ds} = p_u \sin(\theta_{1u}) \qquad if \quad \kappa_{1u} \le \kappa_{cr} \tag{20a}$$

$$\frac{d\kappa_{2u}}{ds} = \frac{1-\alpha}{\alpha} p_i \sin(\theta_{2i}) + p_u \sin(\theta_{2u}) \qquad if \quad \frac{(1+\alpha)}{\alpha}\kappa_{cr} \ge \kappa_{2i} > \kappa_{cr} \tag{20b}$$

$$\frac{d\kappa_{2u}}{ds} = \frac{p_u}{\alpha} \sin(\theta_{2u}) \qquad if \quad \kappa_{2i} > \frac{(1+\alpha)}{\alpha}\kappa_{cr} \tag{20c}$$

The first term on the right-hand-side of equation (20b) indicates that equilibrium depends on the rod configuration when unloading starts. This initial condition was curve fitted with a fourth order polynomial as a function of the rod arc-length. Equations (20a-c) together with the geometrical and compatibility equations (7a-d), which are still applicable, constitute a complex boundary value problem (BVP). The boundary conditions are:

$$x_u(0) = y_u(0) = \theta_u(0) - \beta_u = \kappa_u(0) = \theta_u(1/2) = 0 \tag{20c}$$

An angle controlled solution is developed using a shooting method available in the software Mathcad (2001) through a technique to transform the BVP into an initial value problem. The initial missing value (p_u) is guessed and the boundary value endpoints, set of differential equations and load function returning the initial condition are defined. Next a score function is employed to measure the distance between terminal and desired ($\theta_u(1/2) = 0$) conditions and the equivalent initial condition is obtained. From this point, a Runge-Kutta high order algorithm may be applied to directly integrate the set of non-linear ordinary differential equations.

4. ANALYSIS OF RESULTS

A numerical procedure was developed using the software Matlab (2002) for the loading condition. The analyses were carried out for two non-dimensional critical curvatures, $\kappa_{cr} = 0.5487; 1.6545$, which respectively correspond to end angles $\beta = 10^0; 30^0$. For both cases four reductions in bending stiffness were considered, $\alpha = 1; 0.5; 0.1; 0.01$. For $\alpha = 1$ or when $\kappa_{cr} = 0$ the solution reverts to a full simple elastica since the $M - \mathrm{K}$ relationship is linear. On the other hand when the value of α is reduced higher deviations from the simple elastica solution are expected.

The results for each case listed above are presented in four graphs for free end displacement versus load ($\delta - p$), position of transition point A versus load ($\gamma - p$), end angle versus load ($\beta - p$) and rod maximum deflection versus load ($y_{\max} - p$), respectively depicted in Figures 3a-d and 4a-d for $\kappa_{cr} = 0.5487; 1.6545$. In addition, the simple elastica for $\alpha = 1; 0.5; 0.1; 0.01$ are also plotted in Figure 3a and 4a. The angles β in those figures refer to the post-buckled configurations plotted in Figures 5a-b. The general behaviour for all graphs and both critical curvatures are similar with an expected non-linear response delay (shift) for the higher value of κ_{cr}. Consequently note that for the lower value of κ_{cr} the discrepancies are rather more accentuated. For both cases when the critical curvature is reached the rod becomes more flexible so an immediate initial reduction in load may be observed. This means that if the process is load controlled (see vertical line) a jump phenomenon occurs. For $\beta = 10^0; 30^0$ the rod becomes initially stable, i.e., no jump occurs, roughly for $\alpha \geq 0.976; 0.733$, respectively. The stable window for $\kappa_{cr} = 1.6545$ is somewhat wider since the rod is stiffer, i.e., the inclination of the displacement - load relationship is lower. When unloading, a discontinuous jump may also occur if a bi-linear elastic model is being considered. Note that that the jump is larger for lower values of α in monotonic loading or in elastic reversible processes. Observe that for each combination of κ_{cr} and α there is a minimum value of γ which denotes that part of the rod is subjected to reduction in curvature. Roughly this situation occurred for an end angle approximately equal to 130^o for the range of parameters investigated here. Solution beyond this point was not developed in this paper.

Figures 3a and 4a show that if process is displacement controlled the load reduces to a minimum value and then it grows again. The lower the α the larger is the reduction in load. For the same end angle β the difference in load and end displacement are higher for lower values of α. Furthermore note the uniqueness of the $\delta - p$ relation.

Comparisons between Figures 3b and 4b show that for small values of κ_{cr} or α a longer rod segment is affected. Now note the uniqueness of the $\gamma - p$ relation.

In figures 3c and 4c it is clear that the lower value of κ_{cr} potentially enhances the influence of α. It also indicates the extremity final angle when the rod is post-buckled with load or displacement control. The $\beta - p$ relation is unique.

Figures 3d and 4d indicate that $y_{\max}$ grows with decreasing α for both values of κ_{cr}. The point of maximum displacement β tends 90^0 when α tends to zero, and interesting the load also conveys to a minimum. The function $y_{\max} - p$ presents a non-uniqueness feature.

Figures 5a and 5b display the rod configuration after being monotonically loaded, respectively for $\kappa_{cr} = 0.5487; 1.6545$. Only the half space is plotted since the problem is symmetric. The geometric configurations are presented for $\beta = 10^0; 20^0; 30^0; 60^0; 90^0; 120^0$. If the critical curvature is not exceeded, a solution is obviously given by the linear elastica. It can be seen that the value of the bending stiffness reduction factor significantly influences the rod post-buckled configuration. Observe from Figures 3a-d and 4a-d that these equilibrium configurations are reached with very different parameters $p - \delta - \gamma - y_{\max}$. Another

interesting feature is that the lower the value of α the longer is the "nearly straight" segment, however the rod experiences higher localized curvatures. On the other hand the rod bows "more uniformly" at high values of α.

Figures 6a-c and 7a-c show the geometrical configuration for $\kappa_{cr} = 0.5487; 1.6545$, respectively, and each value of α, when the rod is monotonically loaded until $\beta = 10^0; 20^0; 30^0; 60^0; 90^0; 120^0$ and then the load is completely removed. The final configuration of the first segment, as expected, is a straight line. A reduction in curvature is noticed, but a similar shape pattern is kept. Significant hysteresis is observed for lower values of α, with permanent deflection and little elastic restoration. This characteristic is more pronounced for $\kappa_{cr} = 0.5487$.

Figure 8 presents the geometrical configurations for an unloading process when $\kappa_{cr} = 0.5487$, $\alpha = 0.5$ and initial end angles are $\beta = 30^0; 90^0; 120^0$. It is seen that as the load is removed the curvature reduces but a permanent deformation remains. The parameters governing this unloading process are seen in Figures 9a and 9b, respectively for the curves $\delta - p$ and $\beta - p$. Due to its uniqueness characteristic the unloading can be load or displacement controlled. The less the rod is deflected the higher is the elastic restoring force and the rod tends to return to its original straight configuration.

Table 1 shows the transition curvatures for κ_{cr} and α values employed in this paper. The critical and transition curvatures establish the boundaries for the type of unloading path experienced by a cross-section.

Table 1 - Transition Curvatures

$\alpha \rightarrow$	0.01	0.1	0.5	1.0
$\kappa_{cr} \downarrow$	$\kappa_T \downarrow$			
0.5487	55.4187	6.0357	1.6461	1.0974
1.6545	167.1045	18.1995	4.9635	3.3090

Tables 2a and 2b give the type of unloading path for the cases simulated in this paper, respectively for κ_{cr} = 0.5487 and 1.6545.

Table 2a - Unloading Mechanism for κ_{cr} = 0.5487

$\alpha \rightarrow$	0.01	0.1	0.5
β (deg)$\downarrow$	κ_{cr} = 0.5487		
10	Elastic unloading	Elastic unloading	Elastic unloading
20	Path A	Path A	Path A
30	Path A	Path A	Path B
60	Path A	Path A	Path B
90	Path A	Path B	Path B
120	Path A	Path B	Path B

Table 2b - Unloading Mechanism for κ_{cr} = 1.6545

$\alpha \rightarrow$	0.01	0.1	0.5
β (deg)$\downarrow$	κ_{cr} = 1.6545		
10	Elastic unloading	Elastic unloading	Elastic unloading
20	Elastic unloading	Elastic unloading	Elastic unloading
30	Elastic unloading	Elastic unloading	Elastic unloading
60	Path A	Path A	Path A
90	Path A	Path A	Path B
120	Path A	Path A	Path B

6. CONCLUSIONS

The mathematical formulation for the post-buckling analysis of double-hinged slender rods subjected to compressive axial load and with cross-section bending moment – curvature relationship bi-linear was presented in this paper. This constitutive flexural model may arise from physical or geometrical non-linear characteristics, such as plastic or hyper elastic strains or internal friction mechanisms. Analytical and numerical solutions are respectively developed for monotonic loading and unloading, the former via elliptical integrals whereas the latter one employing transformation of the one point boundary value to an initial value problem through a shooting method. Consequently the hysteresis originating from a complex loading history may be calculated. The variables are made non-dimensional so it is seen that two parameters govern the solutions: the critical curvature κ_{cr} which establishes the transition in the cross-section flexibility and the reduction factor for the bending stiffness α. As the rod post-buckling residual strength is already low, i.e., it can develop large deflections with small increase in load after buckling, it is seen that a reduction in bending stiffness is detrimental to the system stability. For a given critical curvature the range of bending stiffness reduction factor where solution is stable is very narrow. Outside this region the rod is initially unstable so it may jump to another equilibrium configuration if load is progressively applied. When the critical curvature is exceeded and the rod is unloaded the process is not conservative and irreversible yielding permanent deformations. Larger elastic restorations are experienced for larger bending stiffness reduction factors and larger critical curvatures.

The next phase of the work presented here will be to apply the post-buckling methodology to the global in-place analysis of a submerged structure that exhibits bi-linear bending characteristics. The work will follow two lines of enquiry – the first will examine how bi-linear behaviour influences the occurrences of looping and twisting instabilities in structures that have, hitherto, been analysed using linear bending moment relationships. A second line of enquiry will examine the same problem for structures in very deep water where high hydrostatic pressure induces an ‘effective compression’ on such structures.

7. REFERENCES

Costello G.A.: Large deflections of helical spring due to bending, J. of Engineering Mechanics, Div. ASCE. **103**, No.EM3, 481-487 (1977).

Costello G. A., Phillips J. W.: Effective modulus of twisted wire cables, J Engineering Mechanics Div., Proc. ACSE, **102**, 171-181 (1976).

Custódio A. B., Vaz M. A.: A nonlinear formulation for the axisymmetric response of umbilical cables and flexible pipes", Appl. Ocean Research, **24**, 21-29 (2002).

Feld G.: Static and cyclic mechanical behaviour of helically wound subsea power cables, PhD Thesis, Heriot-Watt University (1992).

Feret J. J., Bournazel C. L.: Calculation of stresses and slip in structural layers of unbonded flexible pipes, J. Offshore Mechanics & Arctic Engineering,**109**, 263-269 (1987).

Féret J. J., Leroy J.M., Estrier P.: Calculation of stresses and slips in flexible armour layers with layers interaction, Proceedings of the 14th Offshore Mechanics and Artic Engineering **V**, 469-474 (1995).

Gottlieb O., Perkins N. C.: Local and global bifurcation analyses of a spatial cable elastica. ASME J. Appl. Mech. **66**, 352-60 (1999).

Harte A. M., McNamara J. F.: Verification of analytical modeling procedures for the stress analysis of flexible pipe cross-sections, Proc 9th Int Conf on Offshore Mechanics & Arctic Engineering, Houston, **5**, 99-103 (1990).

Heinen A. H., Fischer O.: Nonlinear vibration and stability analyses on the basis of a kinetic stability theory for arbitrarily curved rods. Archive of Appl. Mech. **68**, 46-63 (1998).

Jurjo D. L. B. R., Gonçalves P. B., Pamplona D.: Large deflection behavior and stability of slender bars under self weight, Proceedings of the 16th Brazilian Congress of Mechanical Engineering, Uberlândia - Brazil (2001).

Knapp R. H.: Non-linear analysis of a helically armoured cable with non-uniform mechanical properties in tension and torsion, Proceedings 1975 IEEE/MTS Conference on Engineering in the Ocean Environment, San Diego, California, 155-164 (1975).

Knapp R. H.: Helical wire stresses in bent cables, ASME J of Offshore Mechanics and Arctic Engineering, **110**, 571-577 (1988).

Knapp R. H.: Structural modeling of undersea cables, ASME J of Offshore Mechanics and Arctic Engineering, **111**, 323-330 (1989).

Koenig H. A., Bolle N. A.: Non-Linear formulation for elastic rods in three-space. Int. J. Non-Linear Mech. **28**, 329-335 (1993).

LeClair R. A., Costello G. A.: Axial, bending and torsional loading of a strand with friction, Proc. 5th Int. Conf. on Offshore Mechanics & Arctic Engineering, Tokyo, 550-555 (1986).

Lee B. K., Wilson J. F., Oh S. J.: Elastica of cantilevered beams with variable cross sections. Int. J. Non-Linear Mech. **28**, 579-589 (1993).

Lee B. K., Oh S. J.: Elastica and buckling load of simple tapered columns with constant volume. Int. J. Non-Linear Mech. **37**, 2507-2518 (2000).

Leroy J.-M., Estrier P.: Calculation of stresses and slips in helical layers of dynamically bent flexible pipes, Oil & Gas Science and Technology – Rev. IFP, **56**, 545-554 (2001).

Love A. E. H.: A treatise on the mathematical theory of elasticity, 4th ed., New York: Dover Publications (1944).

Lu C.–L., Perkins N. C.: Complex spatial equilibria of u-joint supported cables under torque, thrust and self-weight. Int. J. Non-Linear Mech. **30**, 271-285 (1995).

Lutchansky M.: Axial stresses in armour wires of bent submarine cables, J of Engineering for Industry, ASME, 687-693 (1969).

Matlab, Matlab Version 6.5 (2002).

McIver D.: A method of modeling the detailed component and overall structural behaviour of flexible pipe sections, Proc MARINFLEX 92, Bentham Press London (1992).

McNamara J. F., Harte A. M.: Three-dimensional analytical simulation of flexible pipe wall structure, J of Offshore Mechanics & Arctic Engineering, **114**, 69-75 (1992).

Oliveira J. G., de Goto Y., Okamoto T.: Theoretical and methodological approaches to flexible pipe design and application, OTC 5021. Houston, 517-526 (1985).

Out J. M. M.: On the prediction of the endurance strength of flexible pipe, OTC 6165, Houston, 487-496 (1989).

Pearson O. J., Tan Z., Witz J. A.: ABAQUS modelling of a strand - a contact problem, 8th UK ABAQUS User Group Conference, September, Leicester University, Hibbett, Karlesson and Soransen, 66-73 (1993).

Raoof M., Huang Y. P.: Wire stress calculations in helical strands undergoing bending, ASME J of Offshore Mechanics & Arctic Engineering, **114**, 212-219 (1992).

Saevik S.: A method for analysing stresses and slip in flexible pipe armouring tendons at bending gradients, Int Seminar on Flexible Pipe Technology, Marine Technology Centre, Trondheim, Norway, 55-82 (1992).

Seyed F. B., Patel M. H.: Mathematics of flexible risers including pressure and internal flow effects, J. of Marine Structures **5**, 121-15 (1992).

Shames I. H., Dym C. L.: Energy and finite element methods in structural mechanics, 423-428, Ed. Taylor & Francis (1991).

Spillers W. R., Eich E. D., Greenwood A. N., Eaton R.: A helical tape on cylinder subjected to bending, J. of Engineering Mechanics. Div. ASCE, **109**, 1124-1133 (1983).

Stemple T.: Extensional beam-columns: an exact theory, Int. J. Non-Linear Mech. **25**, 615-623 (1990).

Tan Z., Witz J. A.: On the flexural-torsional behavior of a straight elastic beam subject to terminal moments. ASME J. Appl. Mech. **60**, 498-505 (1993).

Tan Z., Witz J. A.: On the deflected configuration of a slender elastic rod subject to parallel terminal forces and moments. Proc. R. Soc. London Ser. **A449**, 337-349 (1995).

Tan Z., Witz J. A., Lyons G. J., Fang J., Patel M. H.: On the influence of internal slip between component layers on the dynamic response of unbonded flexible pipe, Proceedings of the Offshore Mechanics and Arctic Engineering Conf., **1B**, ASME, 563-569 (1991).

Tauchert T. R., Lu W. Y.: Large deformation and postbuckling behavior of an initially deformed rod, Int. J. Non-Linear Mech. **22**, 511-520 (1987).

Theocaris P. S., Panayotounakos D. E.: Exact solution on the non-linear differential equation concerning the elastic line of straight rod due to terminal loading, Int. J. Non-Linear Mech. **17**, 395-402 (1982).

Timoshenko S. P.: Strength of materials - part II, 3rd Ed., D Van Nostrand, New York (1956).

Timoshenko, S. P.: Theory of elastic stability, 4th Edition, McGraw-Hill Book Co. Inc., New York (1964).

Timoshenko S. P., Gere J. M.: Theory of elastic stability, 2nd ed., Singapore: McGraw-Hill International Editions (1961).

Vaz M. A., Silva D. F. C.: Post-buckling analysis of slender elastic rods subjected to terminal forces, Int. J. Non-Linear Mech. **38**, 483-492 (2003).

Wang C. Y.: Post-buckling of a clamped-simply supported elastica. Int. J. Non-Linear Mech. **32**, 1115-1122 (1997).

Witz J. A., Tan Z.: On the axial-torsional structural behaviour of flexible pipes, umbilicals and marine cables, Marine Structures, **5**, 205-227 (1992a).

Witz J. A., Tan Z.: On the flexural structural behaviour of flexible pipes, umbilicals and marine cables, Marine Structures, **5**, 229-249 (1992b).

Yu T. X., Johnson W.: The plastica: the large elastic-plastic deflection of a strut, Int. J. Non-Linear Mech. **17**, 195-209 (1982).

ACKNOWLEDGEMENTS

The authors acknowledge the support from the National Council of Scientific and Technological Development (CNPq) and the National Petroleum Agency (ANP) for this work.

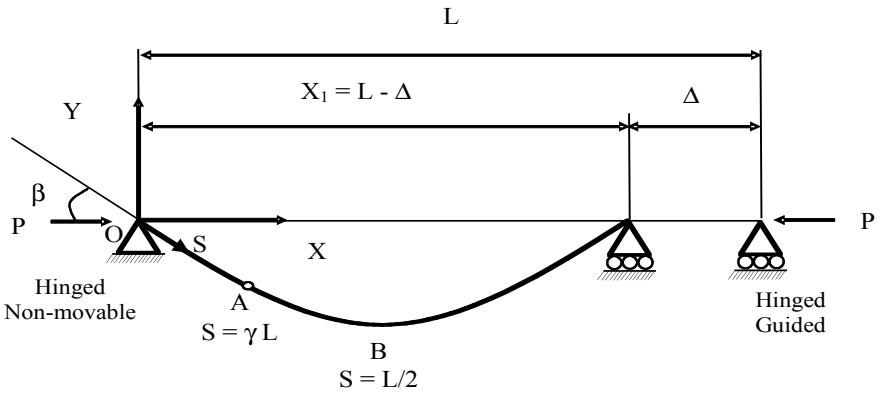

Figure 1a - Schematic of a Post-Buckled Rod.

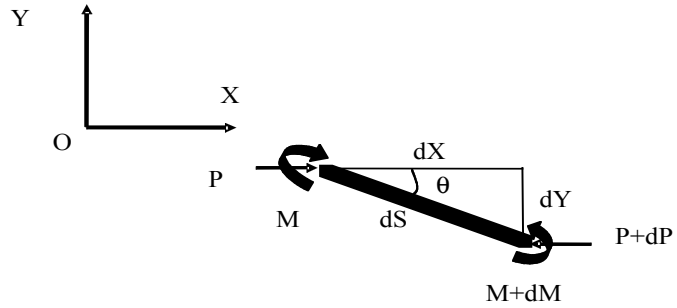

Figure 1b – Infinitesimal Element of Rod.

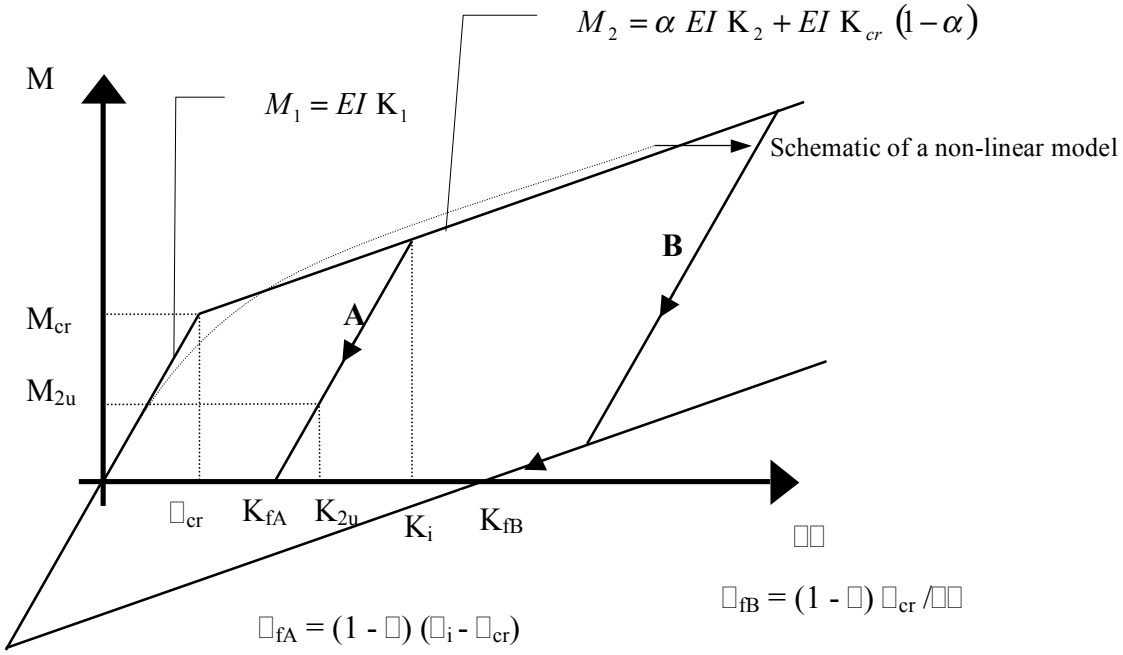

Figure 2 – Cross-Sectional Bi-Linear Bending Moment Versus Curvature.

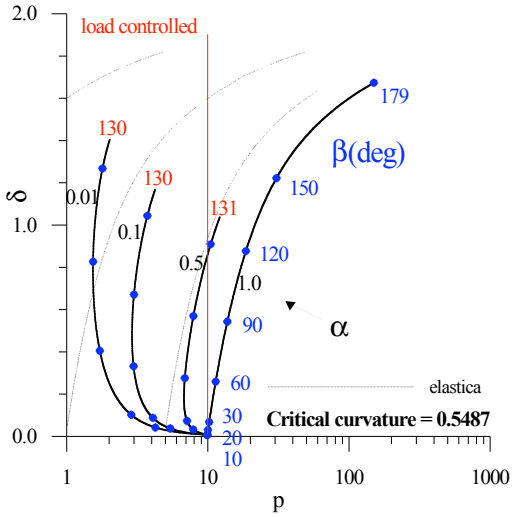

(3a) $\delta - p$

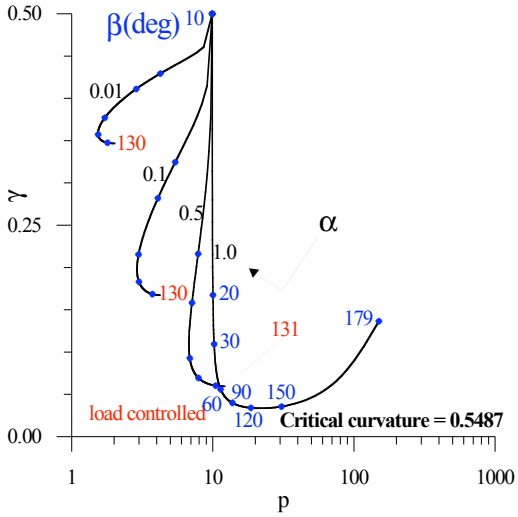

(3b) $\gamma - p$

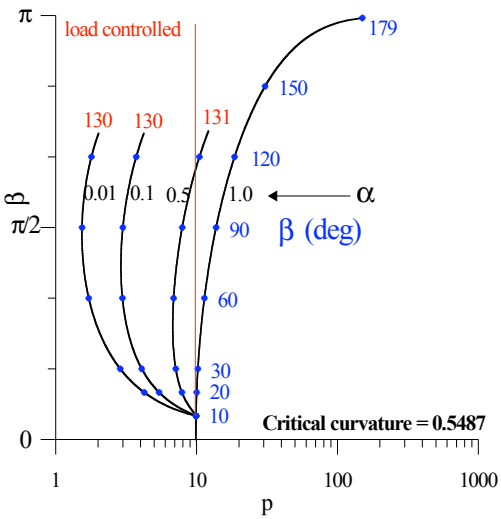

(3c) $\beta - p$

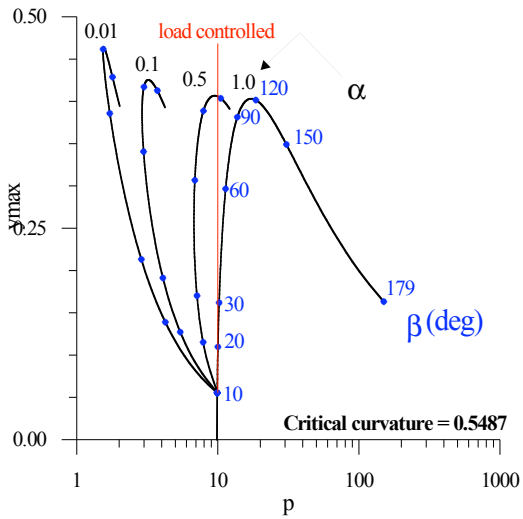

(3d) $y_{\max} - p$

Figure 3 - Post-Buckled Data for $\kappa_{cr} = 0.5487$

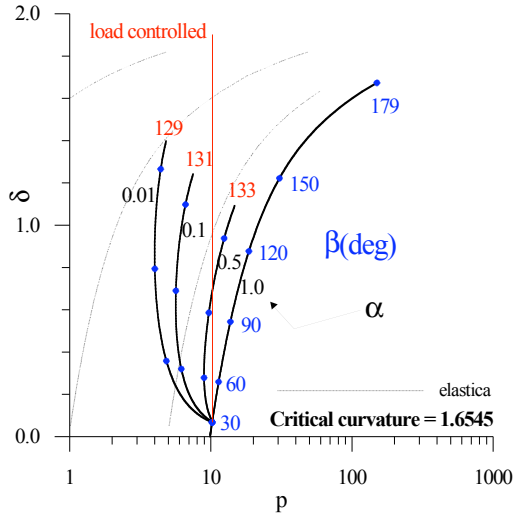

(4a) $\delta - p$

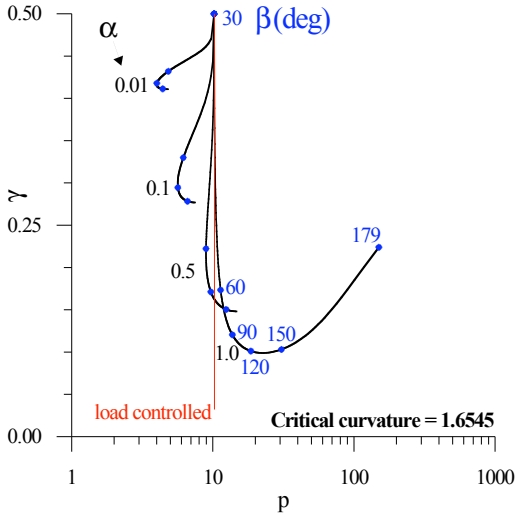

(4b) $\gamma - p$

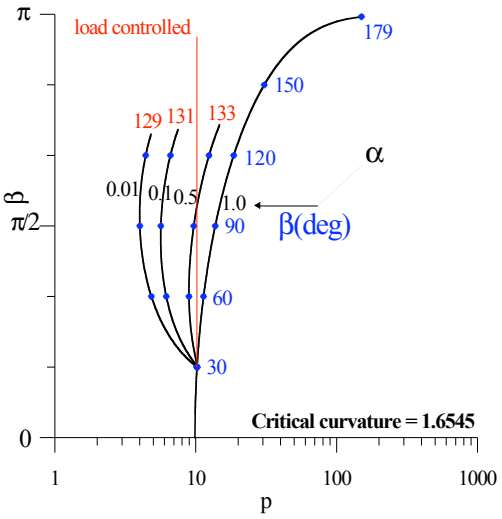

(4c) $\beta - p$

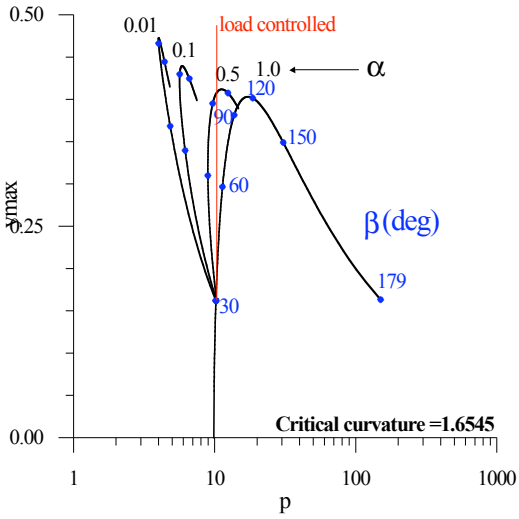

(4d) $y_{\max} - p$

Figure 4 - Post-Buckled Data for $\kappa_{cr} = 1.6545$

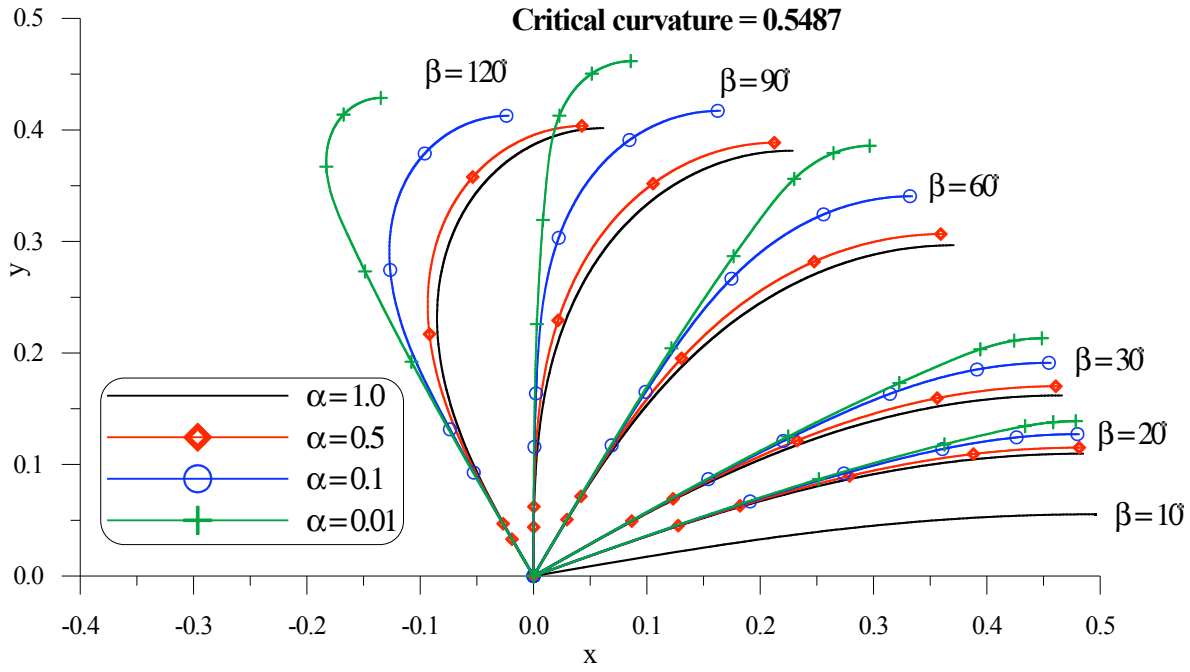

Figure 5a - Rod Post-Buckled Configuration for $\kappa_{cr} = 0.5487$

(Monotonic Loading)

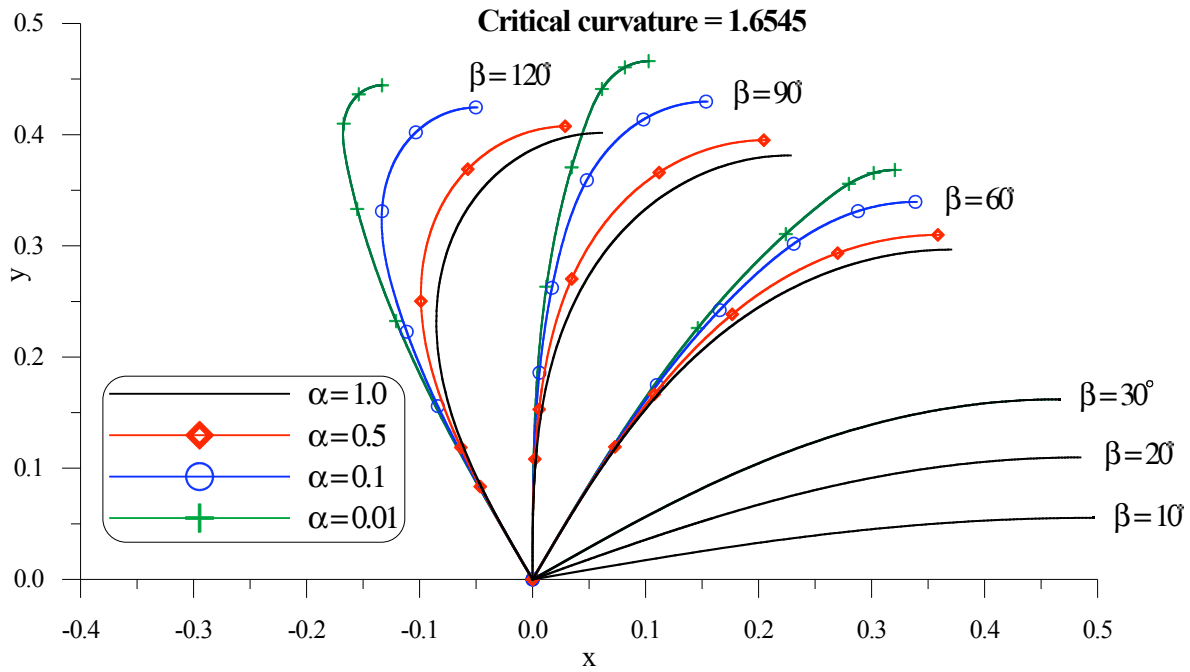

Figure 5b - Rod Post-Buckled Configuration for $\kappa_{cr} = 1.6545$

(Monotonic Loading)

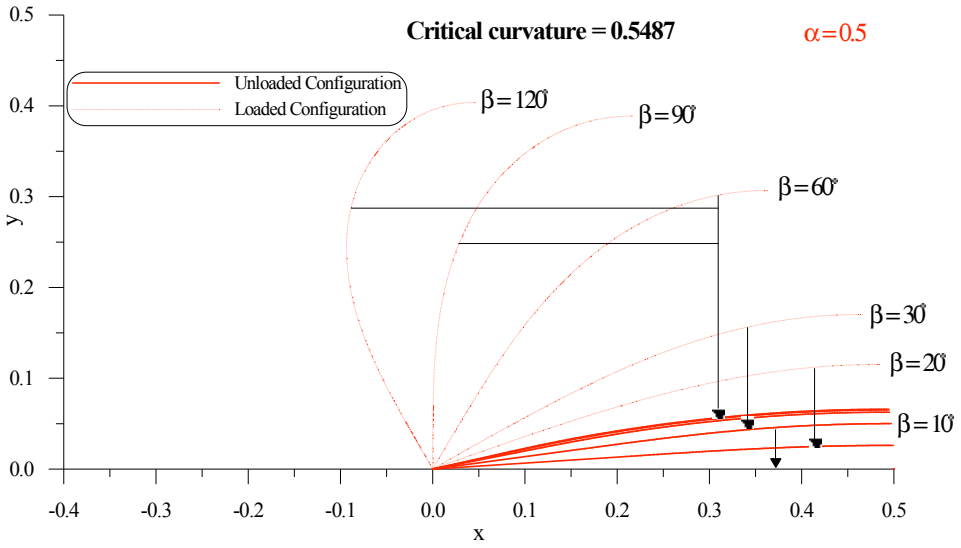

Figure 6a - Rod Post-Buckled Unloaded Configuration for $\kappa_{cr} = 0.5487$ and $\alpha = 0.5$

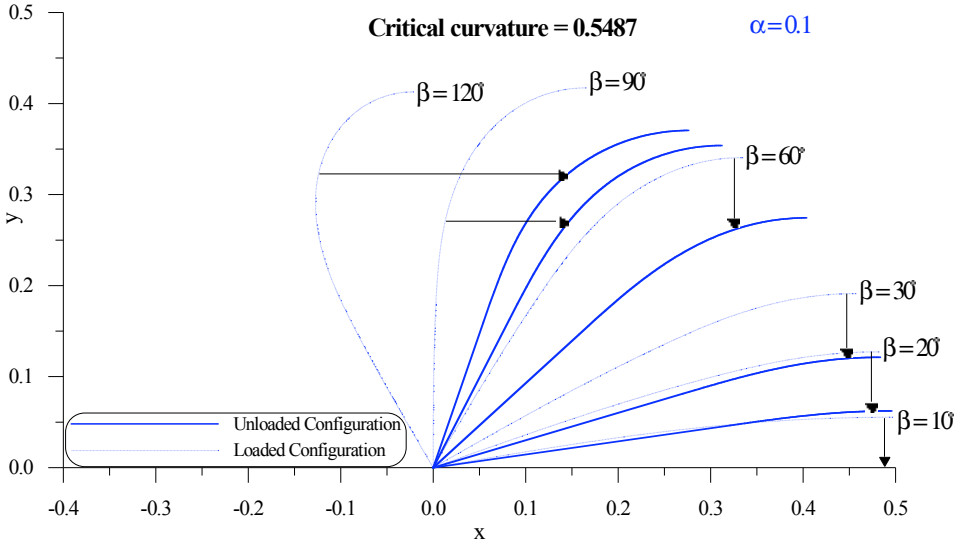

Figure 6b - Rod Post-Buckled Unloaded Configuration for $\kappa_{cr} = 0.5487$ and $\alpha = 0.1$

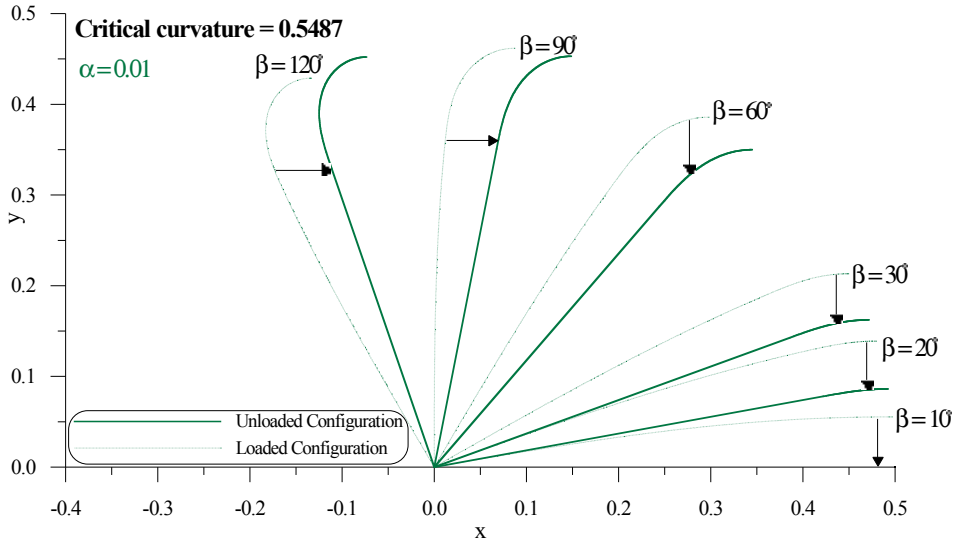

Figure 6c - Rod Post-Buckled Unloaded Configuration for $\kappa_{cr} = 0.5487$ and $\alpha = 0.01$

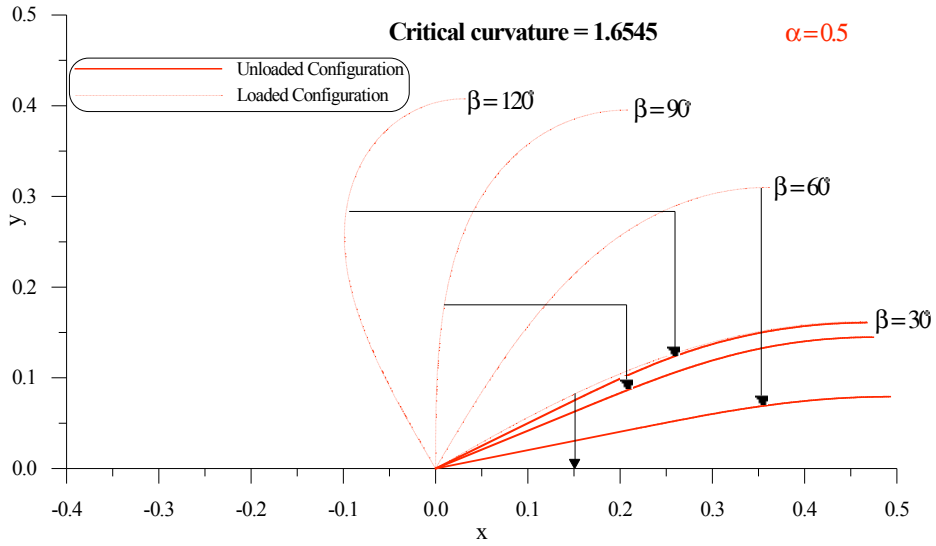

Figure 7a - Rod Post-Buckled Unloaded Configuration for $\kappa_{cr} = 1.6545$ and $\alpha = 0.5$

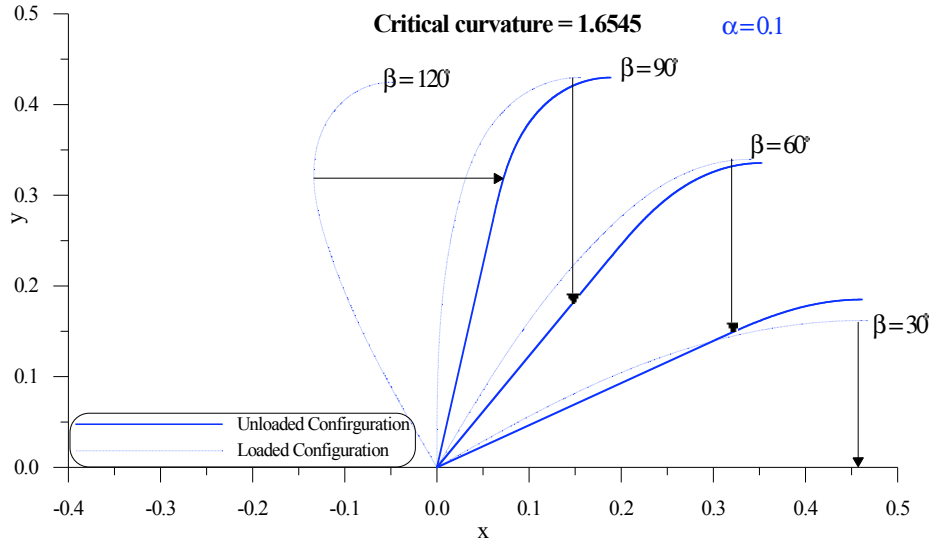

Figure 7b - Rod Post-Buckled Unloaded Configuration for $\kappa_{cr} = 1.6545$ and $\alpha = 0.1$

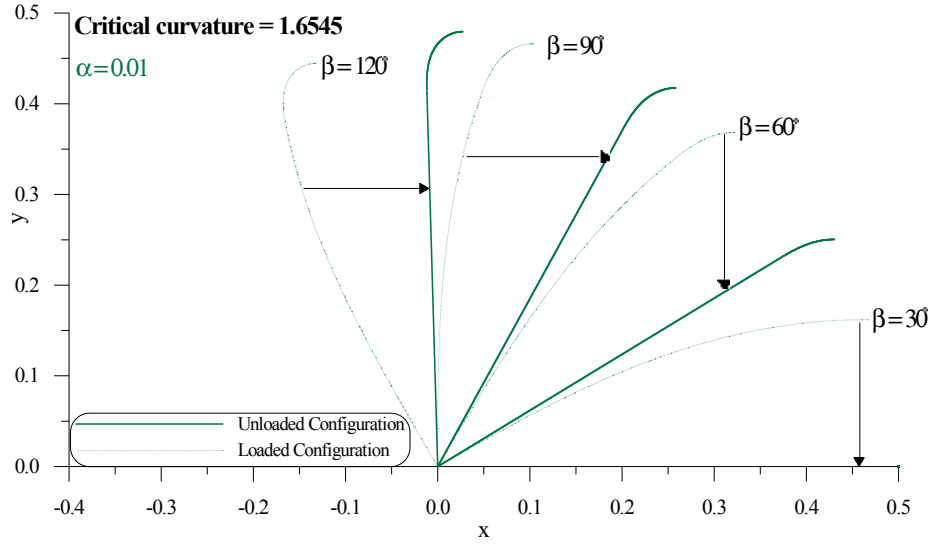

Figure 7c - Rod Post-Buckled Unloaded Configuration for $\kappa_{cr} = 1.6545$ and $\alpha = 0.01$

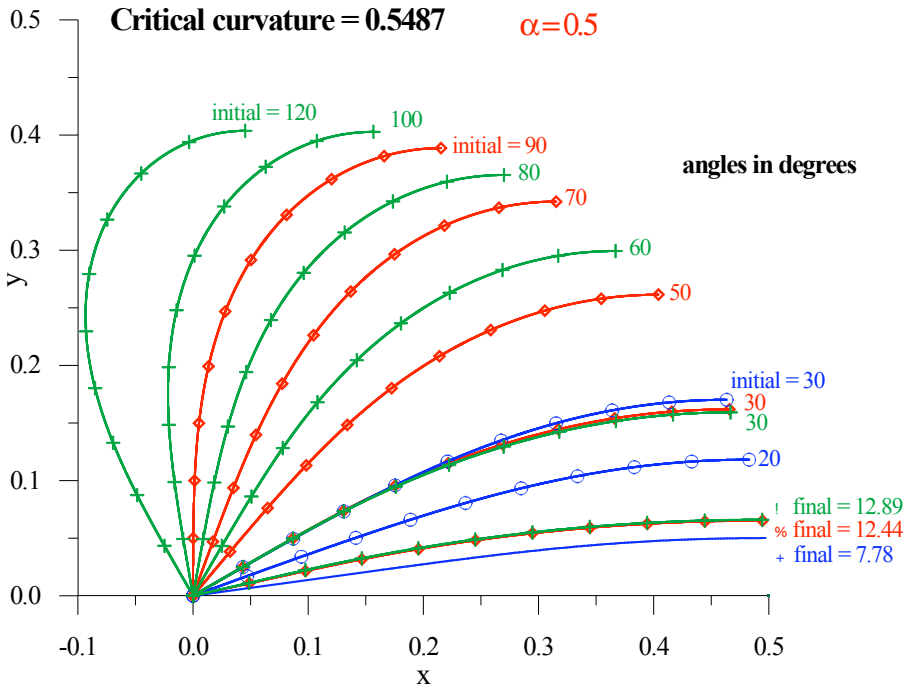

Figure 8 - Rod Post-Buckled Partial Unloading Configurations for $\kappa_{cr} = 0.5487$, $\alpha = 0.5$ and Initial Angles $\beta = 30,90,120\,\text{deg}$

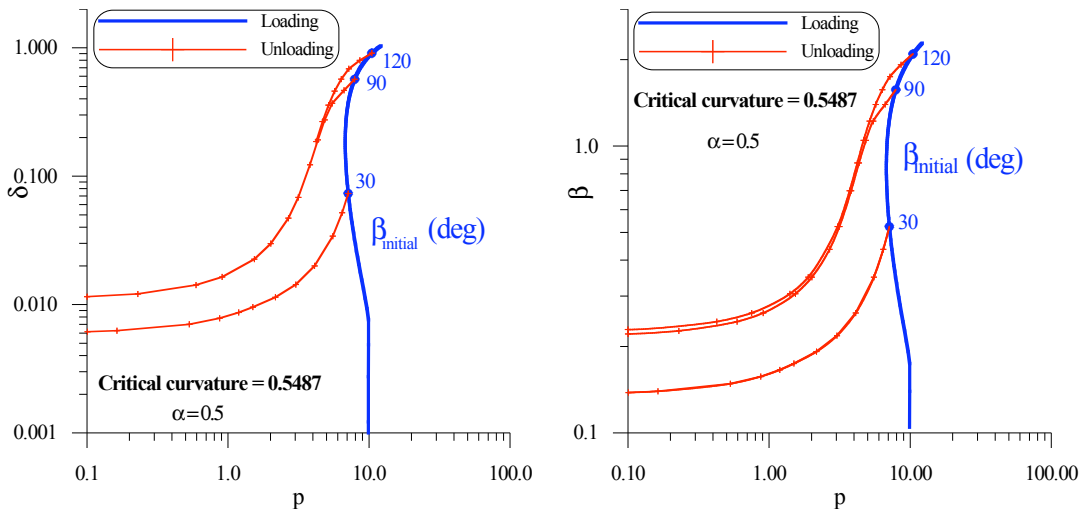

(9a) $\delta - p$ (9b) $\beta - p$

Figure 9 - Unloading Post-Buckled Data for $\kappa_{cr} = 0.5487$, $\alpha = 0.5$ and Initial Angles $\beta = 30,90,120\,\text{deg}$